

Supporting Information

Effective Driving of Ag-loaded Al-doped SrTiO₃ under irradiation at
 $\lambda > 300$ nm for the photocatalytic conversion of CO₂ by H₂O

Shuying Wang[†], Kentaro Teramura^{†,‡*,}, Takashi Hisatomi[§], Kazunari Domen^{§,#}, Hiroyuki Asakura^{†,‡},
Saburo Hosokawa^{†,‡}, Tsunehiro Tanaka^{†,‡*}

[†]Department of Molecular Engineering, Graduate School of Engineering, Kyoto University,
Kyotodaigaku Katsura, Nishikyo-ku, Kyoto 615-8510, Japan

[‡]Element Strategy Initiative for Catalysts & Batteries (ESICB), Kyoto University, 1-30 Goryo-Ohara,
Nishikyo-ku, Kyoto 615-8245, Japan

[§]Research Initiative for Supra-Materials, Shinshu University, 4-17-1 Wakasato, Nagano 380-8553,
Japan

[#]The University of Tokyo, 7-3-1 Hongo, Bunkyo-ku, Tokyo 113-8656, Japan

E-mail: teramura@moleng.kyoto-u.ac.jp

E-mail: tanakat@moleng.kyoto-u.ac.jp

TABLE OF CONTENT

| | |
|--|-----|
| Table S1. BET surface area, FWHM of the {110} diffraction peak, and molar ratio determined by ICP-OES | S3 |
| Figure S1. XPS for pristine SrTiO ₃ , 0 mol% SrTiO ₃ -Y and 0 mol% Al-SrTiO ₃ | S4 |
| Figure S2 SEM images of 0 mol% SrTiO ₃ | S5 |
| Figure S3. UV-Vis DR spectra..... | S6 |
| Figure S4. XRD patterns of Ag/Al-SrTiO ₃ | S7 |
| Table S2. Comparison of the photocatalytic performances | S8 |
| Figure S5. Atomic ratios of Al, Sr, and Ti to the total of Ti and Al | S9 |
| Figure S6. pH value of the suspension solution during photocatalytic reaction..... | S10 |
| Figure S7. Time-dependent evolution of the photocatalytic products | S11 |
| Figure S8. SEM images of Ag/Al-SrTiO ₃ before and after the photoreaction | S12 |
| Figure S9. Emission spectrum of the high-pressure Hg lamp..... | S13 |
| REFERENCE..... | S14 |

Table S1. BET surface area, FWHM of the {110} diffraction peak, Molar ratio, determined by ICP-OES

| Various kinds of catalyst | BET/ $\text{m}^2 \text{ g}^{-1}$ | FMHW | Al / Ti*100 (experiment) (%) | Al/(Al+Ti)*100 (ICP-OES) (%) |
|-----------------------------------|----------------------------------|-------|---------------------------------|---------------------------------|
| Pristine SrTiO_3 | 3.7 | 0.105 | | 0.63 |
| 0 mol % $\text{SrTiO}_3\text{-Y}$ | 1.1 | 0.057 | 0 | 0.68 |
| 0 mol % Al-SrTiO ₃ | 1.8 | 0.053 | 0 | 1.50 |
| 2 mol% Al-SrTiO ₃ | 4.1 | 0.087 | 2 | 1.68 |
| 4 mol% Al-SrTiO ₃ | 4.5 | 0.087 | 4 | 2.16 |
| 16 mol% Al-SrTiO ₃ | 4.1 | 0.087 | 16 | 4.59 |

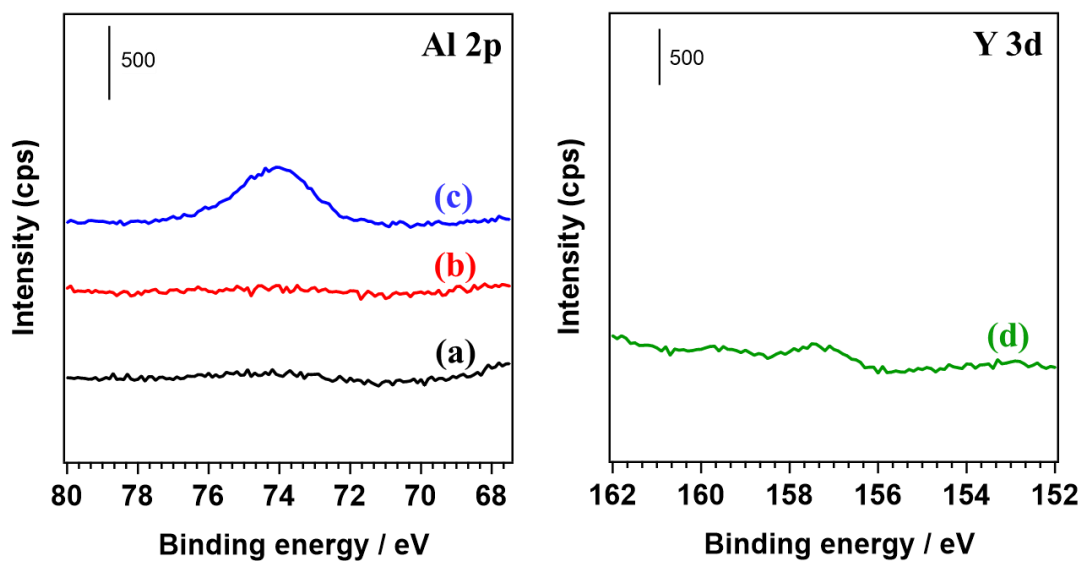


Figure S1. XPS Al 2p for (a) pristine SrTiO₃; (b) 0 mol% SrTiO₃-Y; (c) 0 mol% Al-SrTiO₃; (d) the XPS Y3d for the 0 mol% SrTiO₃-Y.

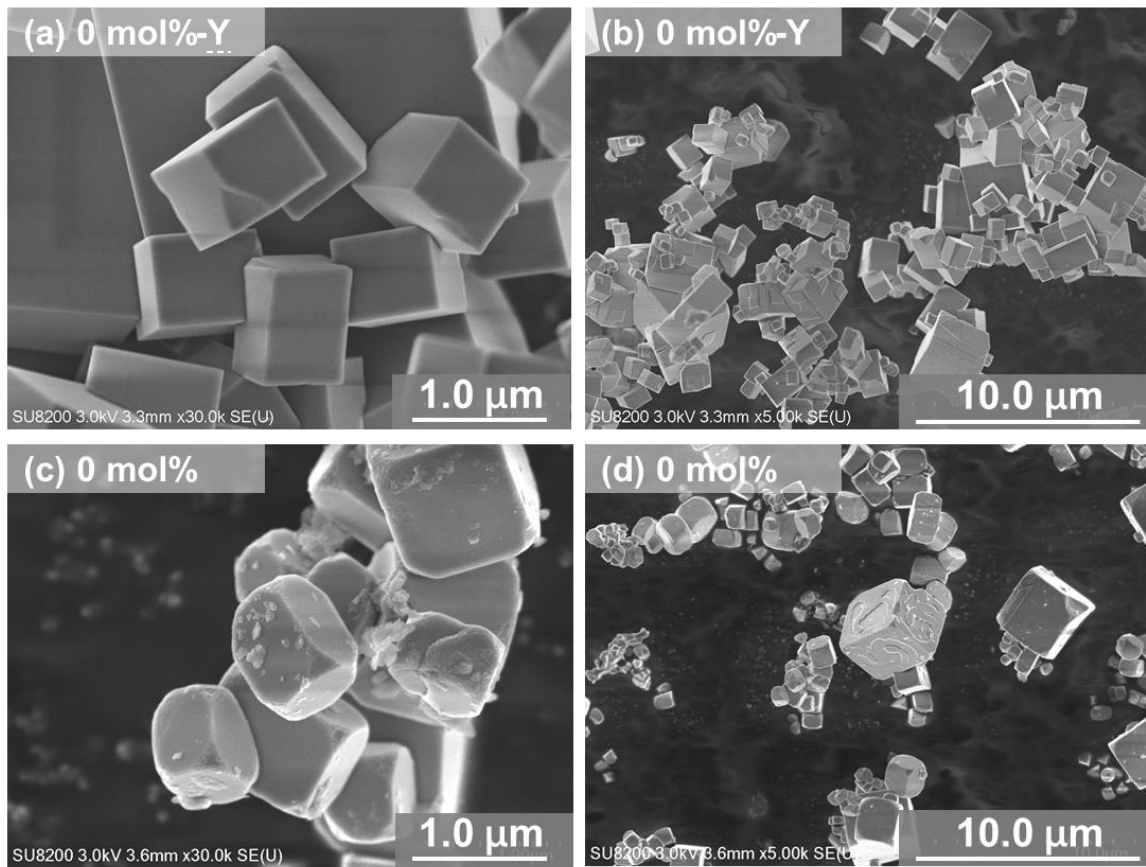


Figure S2. SEM images of (a) and (b) 0 mol% SrTiO₃-Y; (c) and (d) 0 mol% Al-SrTiO₃.

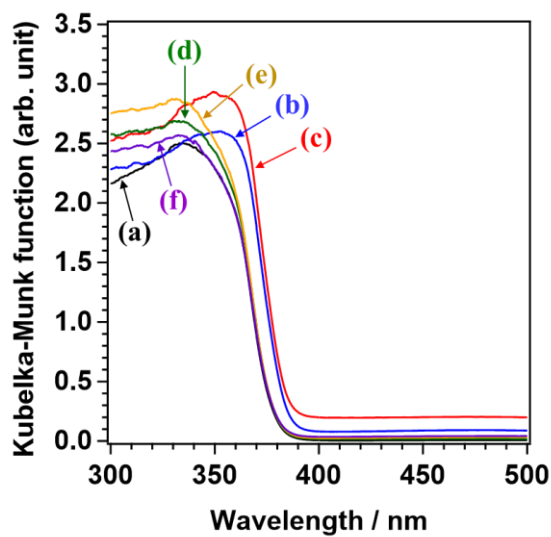


Figure S3. UV-Vis DR spectra of various kinds of SrTiO₃: (a) pristine SrTiO₃; (b) 0 mol% SrTiO₃-Y; (c) 0 mol% Al-SrTiO₃; (d) 2 mol% Al-SrTiO₃; (e) 4 mol% Al-SrTiO₃; and (f) 16 mol% Al-SrTiO₃.

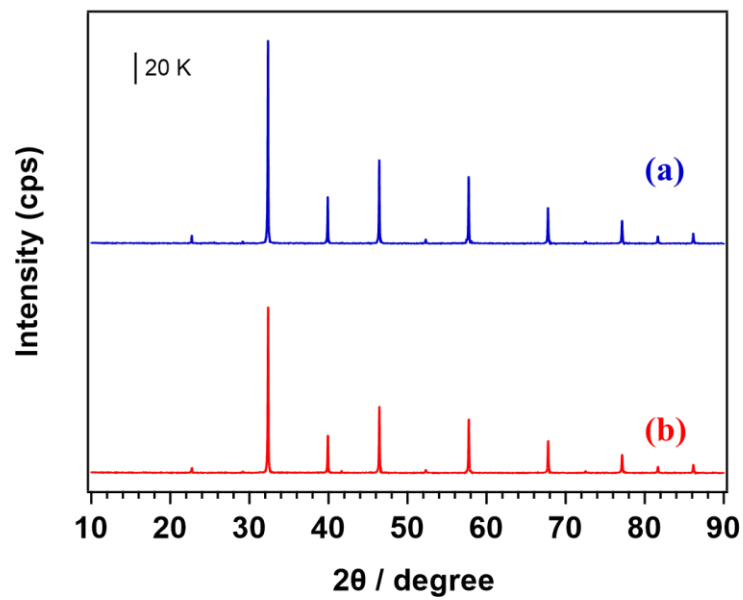


Figure S4. XRD patterns of Ag/Al-SrTiO₃ (a) as-prepared, (b) after 5 hours photoreaction.

Table S2. Comparison of Ag/Al-SrTiO₃ photocatalyst with other CO₂ reduction photocatalysts in aqueous solution under irradiation.

| Catalyst | Formation rates of products ($\mu\text{mol h}^{-1}$) | | | Selec. toward CO (%) | e^-/h^+ | Weight of sample (g) | Solution | Light source Wavelength | Ref. |
|--|--|----------------|------|----------------------------|-----------|-------------------------|---|----------------------------|-----------|
| | H ₂ | O ₂ | CO | | | | | | |
| Ag/SrTiO ₃ | 0.05 | 0.17 | 0.24 | 83.9 | 0.85 | 0.5 | 1.0 L, 0.1M NaHCO ₃ aq. | $\lambda > 300$ nm | This work |
| Ag/Al-SrTiO ₃ | 0.15 | 3.58 | 7.19 | 98.02 | 1.03 | 0.5 | 1.0 L, 0.1M NaHCO ₃ aq. | $\lambda > 300$ nm | This work |
| Ag/BaLa ₄ Ti ₄ O ₁₅ | 10 | 16 | 22 | 67.3 | 1.02 | 0.3 | 0.36 L, aq. | $\lambda > 254$ nm | 1 |
| Ag-Cr/Ga ₂ O ₃ | 92.9 | 281 | 480 | 83.8 | 1.02 | 0.5 | 1.0 L, 0.1M NaHCO ₃ aq. | $\lambda > 254$ nm | 2 |
| Ag-Cr/Ga ₂ O ₃ : Rh | 10.3 | 6.5 | 3.9 | 27.6 | 1.09 | 0.5 | 1.0 L, 0.1M NaHCO ₃ aq. | $\lambda > 300$ nm | 3 |
| Ag/K ₂ YTa ₅ O ₁₅ | 16.3 | 43.2 | 91.9 | 84.9 | 1.25 | 1.0 | 1.0 L, 0.1M NaHCO ₃ aq. | $\lambda > 254$ nm | 4 |
| Ag/SrNb ₂ O ₆ | 1.1 | 24.8 | 51.2 | 97.9 | 1.05 | 0.5 | 1.0 L, 0.1M NaHCO ₃ aq. | $\lambda > 254$ nm | 5 |
| Ag-Mn/K ₂ Ti ₆ O ₁₃ | 0.20 | 4.39 | 10.1 | 98 | 1.17 | 0.3 | 0.4 L, 0.5 M NaHCO ₃ aq. | $\lambda > 254 \pm 10$ nm | 6 |
| Ag/CaTiO ₃ | 0.45 | 0.56 | 0.35 | 44 | 1.5 | 0.2 | 0.01 L, 1.1 M NaHCO ₃ aq. | $\lambda > 254 \pm 10$ nm | 7 |
| Ag/CaTiO ₃ | 3.1 | 25 | 54 | 94 | 1.14 | 0.3 | 0.36 L, 1.0 M NaHCO ₃ aq. | $\lambda > 254 \pm 10$ nm | 8 |
| Ag/Sr-NaTaO ₃ | 28 | 102 | 176 | 86 | 1.0 | 0.2-0.5 | 0.36 L 0.1 M NaHCO ₃ aq. | $\lambda > 254$ nm | 9 |
| Ag/Ca-NaTaO ₃ | 15 | 84 | 148 | 91 | 0.97 | 0.2-0.5 | 0.36 L 0.1 M NaHCO ₃ aq. | $\lambda > 254$ nm | |

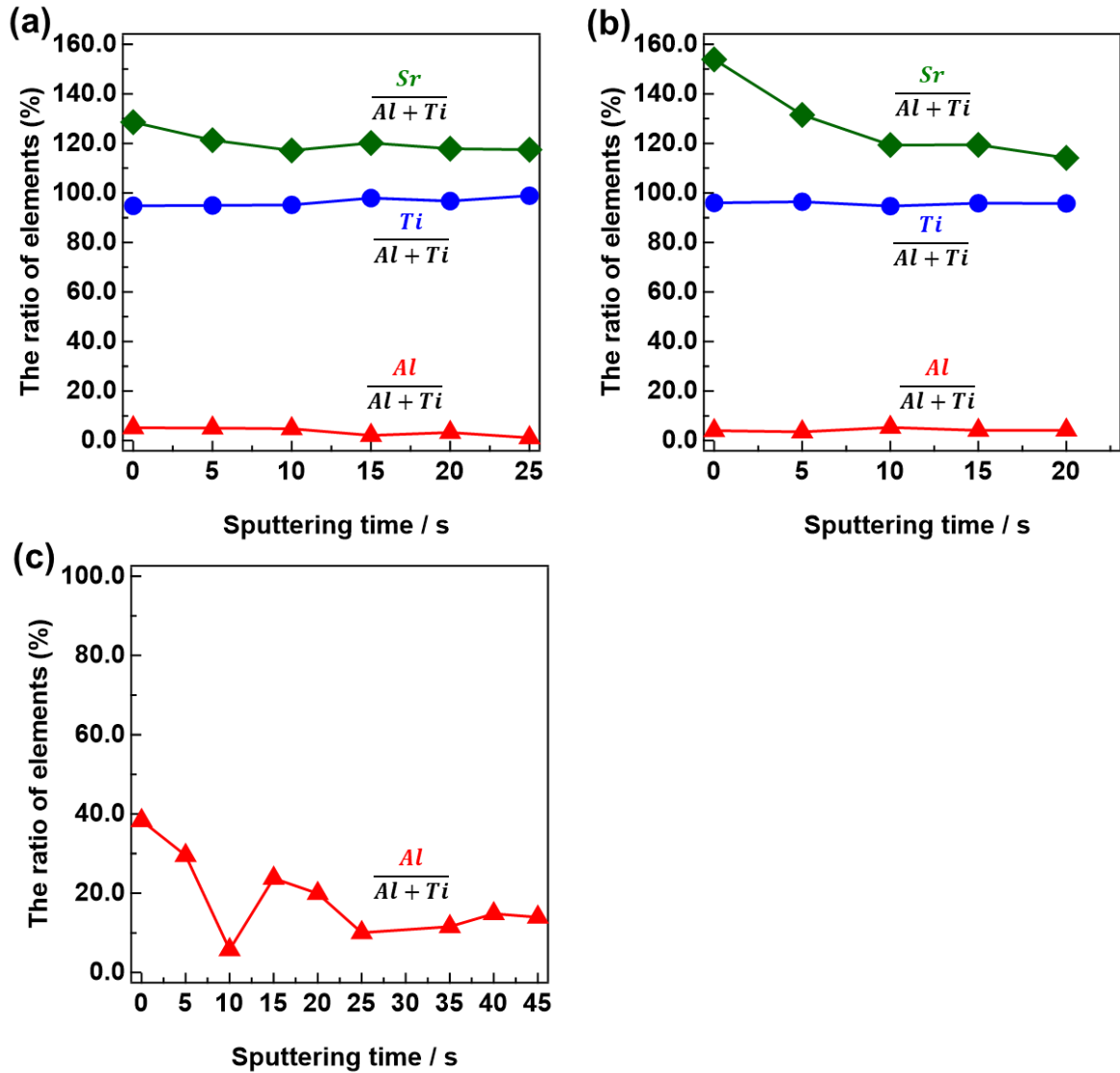


Figure S5. Atom ratio of Al, Sr, Ti elements to the total of Ti and Al; $\text{Sr}/(\text{Al}+\text{Ti})$, $\text{Ti}/(\text{Al}+\text{Ti})$, $\text{Al}/(\text{Al}+\text{Ti})$

(a) pristine SrTiO_3 ; (b) 0 mol% $\text{SrTiO}_3\text{-Y}$; (c) 0 mol% Al- SrTiO_3

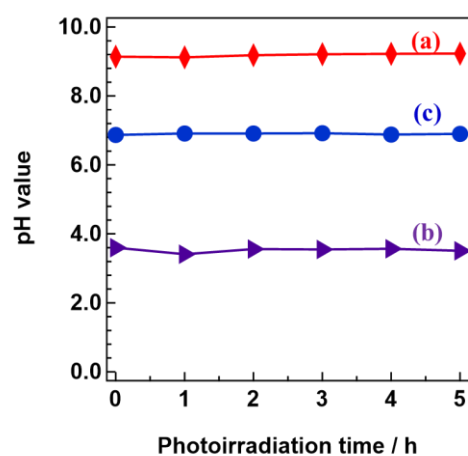


Figure S6. pH value of the suspension solution during the photocatalytic reaction; (a) flowing Ar gas, without a CO₂ gas flow; (b) without the NaHCO₃ additive; (c) typical conditions

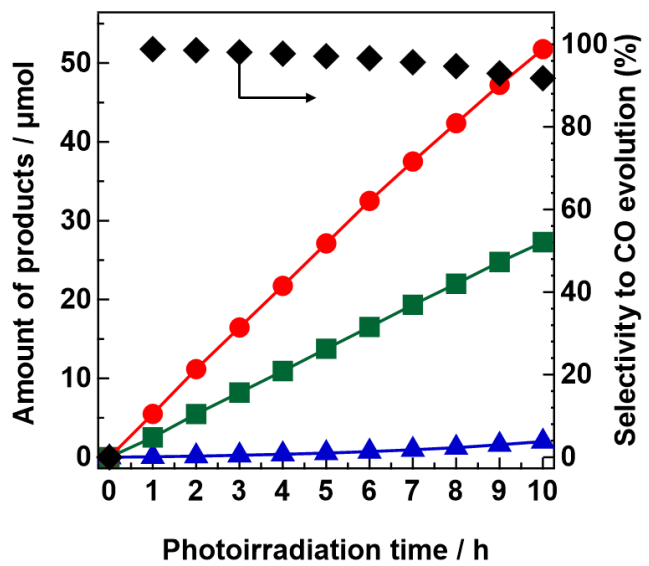


Figure S7. Time-dependent evolution of H₂ (blue triangle), O₂ (green square), CO (red circle), and selectivity to CO evolution (black rhombus) over Ag-loaded Al-SrTiO₃ for 10 h without a break.

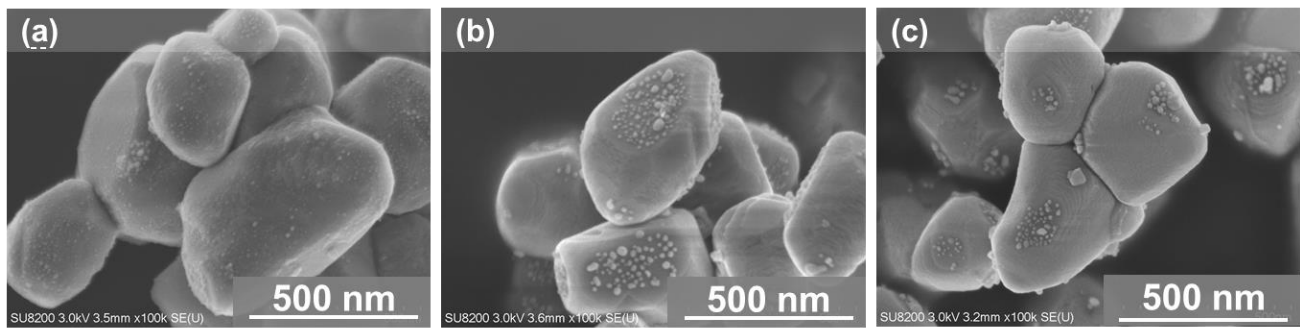


Figure S8 the SEM images of Ag/Al-SrTiO₃; (a) before reaction; (b) after 5 h photocatalytic reaction; (c) after 15 h photocatalytic reaction

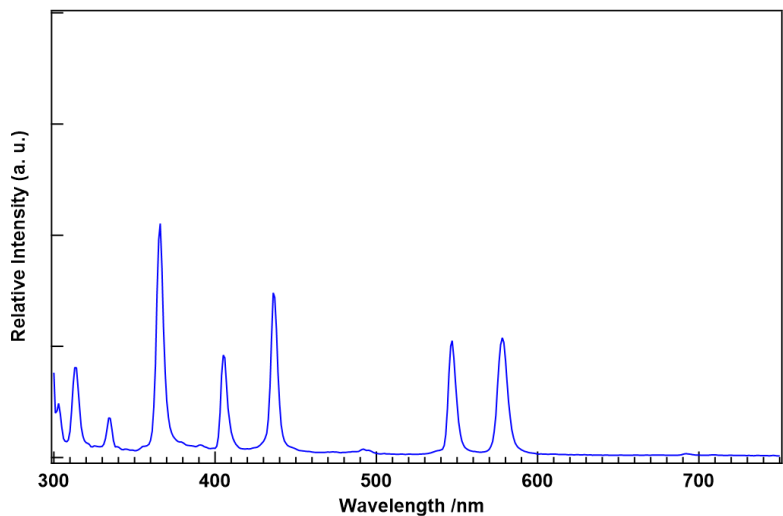


Figure S9. The emission spectrum of high-pressure Hg lamp after Pyrex® cooling jacket.

REFERENCES

- (1) Iizuka, K.; Wato, T.; Miseki, Y.; Saito, K.; Kudo, A. Photocatalytic reduction of carbon dioxide over Ag cocatalyst-loaded $\text{ALa}_4\text{Ti}_4\text{O}_{15}$ (A= Ca, Sr, and Ba) using water as a reducing reagent. *Journal of the American Chemical Society* **2011**, *133* (51), 20863-20868.
- (2) Pang, R.; Teramura, K.; Tatsumi, H.; Asakura, H.; Hosokawa, S.; Tanaka, T. Modification of Ga_2O_3 by an Ag–Cr core–shell cocatalyst enhances photocatalytic CO evolution for the conversion of CO_2 by H_2O . *Chemical communications* **2018**, *54* (9), 1053-1056.
- (3) Kikkawa, S.; Teramura, K.; Asakura, H.; Hosokawa, S.; Tanaka, T. Development of Rh-Doped Ga_2O_3 Photocatalysts for Reduction of CO_2 by H_2O as an Electron Donor at a More than 300 nm Wavelength. *J. Phys. Chem. C* **2018**, *122*, 21132-21139.
- (4) Huang, Z.; Teramura, K.; Asakura, H.; Hosokawa, S.; Tanaka, T. Flux method fabrication of potassium rare-earth tantalates for CO_2 photoreduction using H_2O as an electron donor. *Catalysis Today* **2018**, *300*, 173-182.
- (5) Pang, R.; Teramura, K.; Asakura, H.; Hosokawa, S.; Tanaka, T. Highly Selective Photocatalytic Conversion of CO_2 by Water over Ag-Loaded SrNb_2O_6 Nanorods. *Appl. Catal. B* **2017**, *218*, 770-778.
- (6) Zhu, X.; Yamamoto, A.; Imai, S.; Tanaka, A.; Kominami, H.; Yoshida, H. A Silver-Manganese Dual Co-catalyst for Selective Reduction of Carbon Dioxide into Carbon Monoxide over a Potassium Hexatitanate Photocatalyst with Water. *Chem. Commun.* **2019**, 13514-13517.
- (7) Yoshida, H.; Zhang, L.; Sato, M.; Morikawa, T.; Kajino, T.; Sekito, T.; Matsumoto, S.; Hirata, H. Calcium Titanate Photocatalyst Prepared by a Flux Method for Reduction of Carbon Dioxide with Water. *Catal. Today* **2015**, *251*, 132-139.
- (8) Anzai, A.; Fukuo, N.; Yamamoto, A.; Yoshida, H. Highly selective photocatalytic reduction of carbon dioxide with water over silver-loaded calcium titanate. *Catal. Commun.* **2017**, *100*, 134-138.
- (9) Nakanishi, H.; Iizuka, K.; Takayama, T.; Iwase, A.; Kudo, A. Highly active NaTaO_3 -based photocatalysts for CO_2

reduction to form CO using water as the electron donor. *ChemSusChem* **2017**, *10* (1), 112-118.